PNAS RESEARCH ARTICLE | PLANT BIOLOGY

Age-dependent seasonal growth cessation in *Populus*

Xiaoli Liao[a,b,c,1], Yunjie Su[a,b,c,1], Maria Klintenäs[d,1], Yue Li[a,b,c,1], Shashank Sane[d], Zhihao Wu[a,b,c], Qihui Chen[a,b,c], Bo Zhang[d], Ove Nilsson[d,2], and Jihua Ding[a,b,c,2]

Edited by George Coupland, Max-Planck-Institut fur Pflanzenzuchtungsforschung, Cologne, Germany; received July 3, 2023; accepted October 17, 2023

In temperate and boreal regions, perennial plants adapt their annual growth cycle to the change of seasons. In natural forests, juvenile seedlings usually display longer growth seasons compared to adult trees to ensure their establishment and survival under canopy shade. However, how trees adjust their annual growth according to their age is not known. In this study, we show that age-dependent seasonal growth cessation is genetically controlled and found that the *miR156-SPL3/5* module, a key regulon of vegetative phase change (VPC), also triggers age-dependent growth cessation in *Populus* trees. We show that *miR156* promotes shoot elongation during vegetative growth, and its targets *SPL3/5s* function in the same pathway but as repressors. We find that the *miR156-SPL3/5s* regulon controls growth cessation in both leaves and shoot apices and through multiple pathways, but with a different mechanism compared to how the *miR156-SPL* regulon controls VPC in annual plants. Taken together, our results reveal an age-dependent genetic network in mediating seasonal growth cessation, a key phenological process in the climate adaptation of perennial trees.

tree phenology | age-dependency | bud set | bud break | climate adaptation

Significance

In natural forests, juvenile seedlings display different seasonal growth patterns to adult trees. We characterize the genetic and molecular base of this age-dependent seasonal growth in *Populus* trees. We show a regulatory aspect of the *miR156-SPL3/5s* module in perennial trees that is very different from its mechanism in annual plants. Our study reveals a genetic mechanism for an important climate adaptation, establishment, and survival strategy for trees of different ages in natural forests.

The alteration of periods of active growth and dormancy with the changes of seasonal climate is a widespread adaptive strategy in trees from boreal and temperate regions, which enables them to survive in harsh winter conditions. Photoperiod and temperature are the two main environmental cues regulating the seasonal synchronization of key developmental transitions in the annual growth cycle. In *Populus* trees, autumn shoot growth cessation and bud formation are induced by short days (SDs). Studies have shown that the SD-induced growth cessation is triggered by repression of the expression of the *FLOWERING LOCUS T2* (*FT2*) genes (1, 2). Moreover, recent studies have shown conserved genetic pathways between *Populus* SD–induced growth cessation and photoperiod-controlled flowering time in *Arabidopsis* (3, 4). Tree genes orthologous to genes involved in the *Arabidopsis* photoperiod-controlled flowering time pathway, such as light receptors (*PtPHYA* and *PtPHYB*) (5, 6), circadian clock sensing components (*PtLHYs*, *LATE ELONGATED HYPOCOTYLs*; *PtGI*, *GIGANTEA*) (7, 8), FT2 partner FD-LIKE1 (9, 10), and their downstream target *Like-APETALA1* (*LAP1*) (11), also play roles in SD-induced growth cessation. LAP1 can directly trigger the expression of *AINTEGUMENTA-LIKE 1*, which regulates D-type cyclins to promote cell-cycle progression (12).

After growth cessation, the continuation of SDs induces bud dormancy establishment before winter. Once dormancy is established, buds no longer respond to growth-promotive signals unless exposed to an extended period of cold, following which growth can be reactivated by warm temperature as visibly manifested by bud break. Abscisic acid (ABA) has been reported to play a key role in promoting dormancy establishment by enhancing the biosynthesis and deposition of callose at plasmodesmata to restrict the entrance of growth-promotive signals into shoot meristems (13). Besides, dormancy establishment and dormancy release has been found to be regulated by a group of MIKC-type minichromosome maintenance factor1, agamous, deficiens, serum response factor (MADS)-box transcription factors homologous to the *Arabidopsis* SHORT VEGETATIVE PHASE (SVP)/AGAMOUS-LIKE22 (AGL24) subfamily of MADS-box proteins (14), the central regulators in flowering regulatory networks (15, 16). These genes are referred to as *DORMANCY-ASSOCIATED MADS-BOX*-like in many rosaceous species or *SVP*-like in *Populus* and kiwifruit (17–23). For example, the *Populus SVP* ortholog *SVP-LIKE* (*SVL*) has been reported to not only act as a major hub gene in dormancy induction but also in the regulation of spring bud break (21–23). SVL regulates seasonal growth by antagonistically acting on the ABA and gibberellic acid (GA) pathways, which are the two crucial plant hormones involved in seasonal growth. In addition, *FT1,* another paralog of *FT2,* is strongly induced by cold in the winter (2) and has recently been shown to have a critical role in dormancy release and the regulation of bud break (24, 25). Based on these studies, it is suggested that perennial trees have evolved the ability to integrate the regulation of flowering with the regulation of the seasonal cycling between active and

Author affiliations: [a]National Key Laboratory for Germplasm Innovation and Utilization of Horticultural Crops, College of Horticulture and Forestry, Huazhong Agricultural University, Wuhan 430070, China; [b]Hubei Hongshan Laboratory, Wuhan 430070, China; [c]Hubei Engineering Technology Research Center for Forestry Information, College of Horticulture and Forestry, Huazhong Agricultural University, Wuhan 430070, China; and [d]Department of Forest Genetics and Plant Physiology, Umeå Plant Science Centre, Swedish University of Agricultural Sciences, Umeå 901 83, Sweden

Author contributions: O.N. and J.D. designed research; X.L., Y.S., M.K., Y.L., S.S., Z.W., and Q.C. performed research; X.L., Y.S., Y.L., B.Z., and J.D. analyzed data; and O.N. and J.D. wrote the paper.

The authors declare no competing interest.

This article is a PNAS Direct Submission.

[1]X.L., Y.S., M.K., and Y.L. contributed equally to this work.

[2]To whom correspondence may be addressed. Email: Ove.Nilsson@slu.se or jihuading@mail.hzau.edu.cn.

This article contains supporting information online at https://www.pnas.org/lookup/suppl/doi:10.1073/pnas.2311226120/-/DCSupplemental.

Published November 22, 2023.

dormant vegetative growth through common genes and signal cascades (4).

Besides their polycarpic growth habits, perennial woody plants experience a long period of vegetative growth (including juvenile and adult vegetative growth) before reproductive onset. For example, it will take 5 to 20 y for seed-grown *Populus* trees until onset of flowering (26). Hybrid poplar (*Populus tremula x alba*, clone 717-1B4) trees originating from tissue culture explants will initiate flowering earlier, but not before 3 to 4 y after transplanting. Such a long period of vegetative growth is accompanied by alternations in both plant morphology and physiology to ensure adaptability to environmental changes (27). For example, in a deciduous forest, juvenile and adult trees usually display different phenology patterns to ensure that juvenile trees can maximize carbon gain by extending their first growing seasons to firmly establish themselves and avoid canopy shade. Compared to adult trees, juvenile trees have been found to have a longer growth season by flushing their buds earlier in spring and/or initiating senescence later in fall (28, 29), suggesting that seasonal growth phenology may be affected by the age of the plant (30). However, solid genetic evidence is lacking, and the molecular mechanism underlying this phenological differences between juvenile and adult tree species is unknown.

It is known that the juvenile to adult phase change (vegetative phase change, VPC) is mainly controlled by the microRNA *miR156*, and its roles in the control of VPC appear to be conserved in almost all major plant taxa that have been studied, including *Populus* trees (31–34). As plants age, a gradual decline in *miR156* abundance occurs coupled to a cumulative accumulation of its target SQUAMOSA PROMOTERBINDING PROTEIN (SBP)-LIKE (SPL) transcription factors (35, 36). Furthermore, the reduction of the *miR156* level is coupled with the gradual accumulation of another microRNA, *miR172*, which can repress *APETALA2* (*AP2*)*-like* transcription factors in *Arabidopsis* (37). The expression of *SPL* and *AP2-like* genes is regulated by diverse flowering signals, and they work together concertedly to regulate VPC and flowering initiation (35, 38). In annual plants, the *miR156/miR172* module shows a strong connection between VPC and reproductive competence, which is well known as age-dependent flowering regulation (38). Since *Populus* flowering regulation and the annual cycle of active-dormant growth regulation share common signaling cascades that converge on the *FT*-like genes, we hypothesized that *Populus miR156* and its targets are involved in regulating *FT* expression in leaves that leads to changes in the timing of growth cessation and bud set at different tree ages. To confirm this, we characterized the functions of *miR156* and its targets *SPL3/5s* in regulating seasonal growth cession in hybrid aspen. We show that *miR156* functions as a positive regulator of seasonal active growth and its targets *SPL3/5s* play roles in the same pathway, but as repressors. We have also deciphered the molecular pathways downstream of the *miR156-SPL3/5s* regulon. Our results reveal an age-dependent genetic network mediating seasonal growth cessation, a key phenological process in perennial trees.

Results

Seasonal Growth Cessation Is Associated with Age in *Populus* Trees. It has been shown that aspects of the seasonal growth–dormancy cycle, like the timing of bud set and bud flush, are affected by the age of the tree, but this effect has never been studied systematically (28–30). To this end, we compared the timing of bud set among different ages of hybrid poplar trees (*P. tremula x alba*, clone 717-1B4) grown under natural field conditions. The results confirmed that older trees set bud later than younger trees. The 4-y-old trees set bud on average 12 d earlier than 2-y-old trees (Fig. 1 *A* and *B*), but the bud set was similar in trees older than 3 y (Fig. 1 *A* and *B*). As *miR156* is considered an age marker that regulates juvenile phase change in poplar (34), we checked the expression level and pattern of *miR156* from leaves collected from current-year branches of 2-y and 4-y-old hybrid poplar, respectively. The *miR156* abundance gradually increased

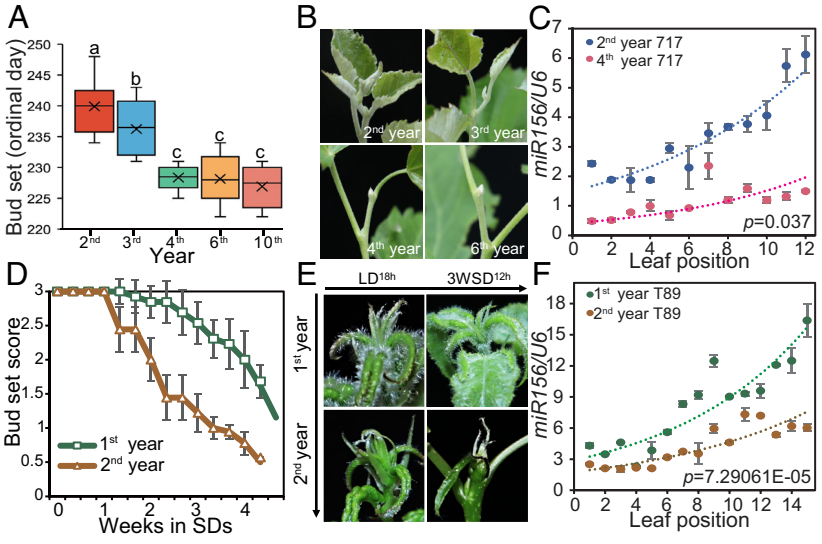

Fig. 1. Seasonal growth cessation is associated with age in *Populus*. (*A*) Bud formation time of field-grown hybrid poplar trees (INRA717-1B4, 717) of different ages. Data shown are mean values of 12 branches from 4 to 6 trees for each age group. Error bars ± SD. Numbers represent the ordinal day number. Different letters represent significant differences from each other as determined by one-way ANOVA with Tukey's multiple comparisons test, $P < 0.05$. (*B*) Shoot apex morphologies of 2-, 3-, 4-, and 6-y-old hybrid poplars on ordinal day 229. (*C*) Expression levels and patterns of mature *miR156* in 2-y and 4-y-old hybrid poplar leaves. (*D*) Bud set score of 1st- and 2nd-year hybrid aspen (T89) trees grown in controlled conditions. Bud set scoring is described in detail in *SI Appendix*, Materials and Methods. Score 1, active growth; score 2, growth cessation; score 3, bud set. Data shown are mean ± SD (n = 6). (*E*) Shoot apex morphologies of 1st- and 2nd-year hybrid aspen trees taken at LD^{18h} and 3 wk after SD^{12h} treatment. (*F*) Expression levels and patterns of mature *miR156* in 1st- and 2nd-year hybrid aspen leaves. The collection of leaf samples used in (*C*) and (*F*) is described in detail in *SI Appendix*, Materials and Methods. 1 (*Top*)–12/15 (*Bottom*): leaf order from current-year long apical branches. Data shown in (*C*) and (*F*) are mean ± SD (n = 3). *P*-values shown in (*C*) and (*F*) represent the significance of differences between 2- and 4-y-old 717, and 1- and 2-y-old T89 as determined by Student's *t* test (pairwise).

from the apical newly formed leaf ("1" in Fig. 1*C*) to the basal fully developed leaf ("12" in Fig. 1*C*) in both the 2-y and 4-y tree branches. Furthermore, the overall expression of *miR156* declined with age, with a remarkable decrease in the relatively older 4-y tree branches (Fig. 1*C*). We also found that in hybrid aspen trees (*P. tremula x tremuloides,* T89) grown under controlled greenhouse conditions, the 2nd-year trees showed a week earlier growth cessation and bud set following a shift from LD^{18h} to SD^{12h} conditions, compared to 1st-year trees (Fig. 1*D*). The 2nd-year tree shoot apices initiated bud set 3 wk after shifting to SD^{12h}, while the 1st-year tree shoot apices were still in active growth (Fig. 1*E*). Consistently, also in these controlled conditions, the expression level of *miR156* declined with the age of trees (Fig. 1*F*), as observed under field conditions (Fig. 1*C*). Taken together, field and greenhouse results suggest that the seasonal growth cessation varies with age in poplar and that the juvenile trees extended their active growth and delay growth cessation compared to older trees.

Altered *miR156* Expression Affects Growth Cessation and Bud Set in Hybrid Aspen Trees. Since *miR156* has been shown to be a key regulator of the juvenile-to-mature VPC in many plant species, including poplar (34), it is a strong candidate also for the regulation of age-dependent seasonal growth cessation. We identified twelve *miR156* loci in the *Populus trichocarpa* genome. The *miR156* mature sequences clustered in three groups (*SI Appendix*, Fig. S1*A* and Table S1). Based on the annual transcriptome data of aspen trees (21), seven primary transcripts of *ptc-MIR156s* were identified and displayed seasonal-specific expression patterns, with most of them showing peaks of expression during summer and early autumn (*SI Appendix*, Fig. S1*B*). In *Arabidopsis*, *ath-MIR156a* and *ath-MIR156c* play dominant roles in VPC (39–41). Thus, we selected *Populus ptc-MIR156c* and *ptc-MIR156e* for further analysis, both of which clustered together with *ath-MIR156a* and *ath-MIR156c* (*SI Appendix*, Fig. S1*A*). Constitutively expressed c or e isoforms of *miR156* were generated by transforming wild-type hybrid aspen (WT, T89) trees with constructs containing a 142-bp or 167-bp stem-loop fragment driven by the constitutive Cauliflower Mosaic Virus *35S* promoter (*SI Appendix*, Figs. S1*C* and S2 *A*–*C*). When potted in the greenhouse, transgenic plants expressing *ptc-MIR156c* or *ptc-MIR156e* exhibited similar phenotypes: reduced plastochron leading to more internodes formed; more sylleptic branches and enlarged leaf-like stipules (*SI Appendix*, Fig. S2 *D* and *E*), similar to what has been described for *Arabidopsis ath-MIR156f* (42). Compared to plants expressing *ptc-MIR156c*, the phenotype of *ptc-MIR156e*-expressing plants (miR156eOE) was relatively stronger. We therefore focused our investigation on the miR156eOE plants (*SI Appendix*, Fig. S2). WT and three independent transgenic lines were potted under LD^{18h} growth conditions for two months and then shifted to SD^{12h} growth conditions. WT plants ceased growth three weeks after the shift to SD (Fig. 2 *A* and *B*). However, the miR156eOE plants displayed hyposensitivity to the daylength shift and started growth cessation about two weeks later compared to the WT (Fig. 2 *A* and *B*). As perception of SDs results in termination of leaf formation, the number of newly formed leaves after exposure to SDs until growth cessation provides a sensitive measure of the SD response (43). At the end of the LD treatment, miR156 OE plants had produced 50% more leaves than the WT due to a lower plastochron (Fig. 2*C*), as has also been reported for *Arabidopsis* (42). In SDs, miR156eOE plants continued to grow and produced on average twice the number of new leaves before bud formation compared to WT plants (Fig. 2*C*). Moreover, transgenic hybrid aspen plants in which the activity of miR156 was suppressed by constitutive expression of a mimic transcript with a noncleavable *miR156* target site (STTM156) were also generated and scored for growth cessation (*SI Appendix*, Fig. S3). In contrast to miR156eOE, STTM156 lines showed earlier growth cessation compared to the WT hybrid aspen plants (Fig. 2 *A* and *B*). Consistently, STTM156 lines produced relatively fewer new leaves after SD treatment than the WT controls (Fig. 2*C*). Our results strongly suggest that *miR156* functions as a repressor of seasonal growth cessation in hybrid aspen.

We also monitored the timing of bud break in miR156eOE and STTM156 plants in controlled climate growth rooms that simulate winter conditions to release dormancy followed by simulated spring conditions to stimulate bud break (*SI Appendix*, Fig. S4*A*). Under these conditions, miR156eOE plants displayed

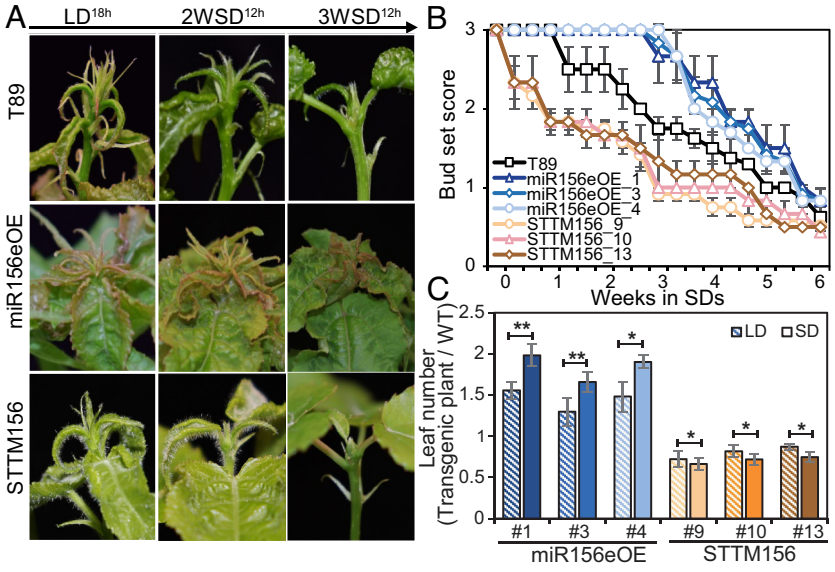

Fig. 2. Altered *miR156* expression affects growth cessation in hybrid aspen. (*A*) Delayed and early growth cessation in miR156eOE and STTM156 plants. Representative shoot apex morphologies of wild-type (T89), miR156eOE, and STTM156 plants taken at LD^{18h} and after 2 and 3 wk of SD^{12h} treatment. (*B*) Bud set score of T89, miR156eOE, and STTM156 plants after transfer from LD^{18h} to SD^{12h} conditions. (*C*) Relative number of new leaves produced under LD^{18h} and SD^{12h} conditions in miR156eOE and STTM156 lines compared to wild-type plants. Data shown in (*B*) and (*C*) are mean ± SD (n = 6 to 8). Asterisks denote significant differences of the leaf initiation ratio (transgenic plants/WT) between LD and SD conditions (*$P < 0.05$, **$P < 0.01$; Student's *t* test).

an earlier bud break (*SI Appendix*, Fig. S4 *B* and *C*), while STTM156 plants were delayed compared to the WT (*SI Appendix*, Fig. S4 *D* and *E*). Taken together, our results suggest that *miR156* can modulate the length of the growing season both by repressing growth cessation in the fall and by promoting bud break in the spring.

***miR156* Mediates Growth Cessation in Both Leaves and Shoot Apices in Hybrid Aspen.** In *Populus*, vegetative growth is maintained by the expression of the *FT2* genes in leaves and the subsequent translocation of the FT2 protein to the shoot apices (44). Autumnal growth cessation is then triggered by shortening daylengths, sensed by phytochrome photoreceptors in leaves, to repress the expression of *FT2* (1, 9, 44). In *Arabidopsis*, *miR156* and its target *SPL* genes have been widely shown to regulate flowering by acting both in the leaf and shoot apex (45–47). To check whether *miR156* was involved in photoperiod-dependent growth cessation or tissue-specific functions in *Populus*, we checked the photoperiod response of *miR156* expression both in leaves and shoots. *miR156* is expressed in both tissues but with significantly lower expression levels in the shoot apex (*SI Appendix*, Fig. S5*A*). There was no significant photoperiod response in the expression of *miR156* either in leaves or shoots (*SI Appendix*, Fig. S5*A*), suggesting that *miR156* may regulate growth cessation in a photoperiod-independent pathway. To investigate whether *miR156* regulates growth cessation in the leaves and/or shoot apex, we grafted WT scions onto WT rootstocks, WT scions on miR156eOE rootstocks, and miR156eOE scions onto WT rootstocks, and then assessed shoot growth of the grafts after exposure to SDs (*SI Appendix*, Fig. S5 *B* and *C*). Both apices of miR156eOE scions grafted onto WT root stocks and apices of WT scions grafted onto miR156eOE root stocks ceased growth in response to SDs later than counterparts grafted on WT (*SI Appendix*, Fig. S5 *B* and *C*). These results suggested that miR156 can not only influence growth cessation by acting in leaves but can also function locally in the shoot apex.

Extensive Changes in Leaf and Shoot Apex Transcriptomes of miR156eOE Plants before and after Growth Cessation Are Triggered. To explore possible regulatory pathways of *miR156*, we performed transcriptome analysis of miR156eOE transgenics together with WT plants using leaves and shoot apices collected under LD^{18h} conditions. A total of 867 and 1,796 differentially expressed genes (DEGs) were identified in leaves and shoot apices respectively, and more DEGs were downregulated in miR156eOE plants (*SI Appendix*, Fig. S6*A* and Dataset S1 *A* and *D*). Gene Ontology analysis indicated that upregulated genes were mainly associated with active growth processes such as meristem activity, GA signaling pathways and auxin signaling, etc. Downregulated genes were mainly involved in defense response or abiotic stress–related phytohormone responses such as ABA, ethylene, jasmonic acid, and salicylic acid responses. Besides, many genes related to flower development were also downregulated, suggesting a possible conserved role in flowering regulation of *miR156* in *Populus* (*SI Appendix*, Fig. S6*A* and Dataset S1 *B* and *E*).

To investigate the relevance of these DEGs to growth cessation, we compared the analysis of DEGs identified in the present study and previously identified DEGs in wild-type leaves and shoot apices before and after 2 wk of SD treatment (referred to as Growth Cessation-associated Genes, GCGs; Dataset S1 *C* and *F*) (5). We found that there were 139 and 150 DEGs [representing 13.8% (139/1,008) and 43.0% (150/349) of all GCGs genes] that were up- or down-regulated in miR156eOE plants in leaves and shoot apices, respectively (*SI Appendix*, Fig. S6*B*). Consistent with the delayed growth cessation phenotype of the miR156eOE plant, almost all these genes, 139 and 150 DEGs/GCGs in leaves and shoot apex, respectively, displayed opposite expression trends compared to their SD responses (*SI Appendix*, Fig. S6*B* and Dataset S1*G*). These results suggest that changes in *miR156* expression extensively affected genes associated with growth cessation. Intriguingly, we found that many genes that control meristem activity were either up- or down-regulated in miR156eOE plants, such as *SHOOTMERISTEMLESS* (*STM*), *KNOTTED1-LIKE HOMEOBOX GENE 6* (*KNAT6*), and *CLV3/ESR-related* genes (*CLEs*) (*SI Appendix*, Fig. S6*C*). Three *SVP/AGL24-like* genes were also found to be down-regulated in miR-156eOE plants (*SI Appendix*, Fig. S6*C*, named *SVL2, SVL5,* and *SVL6* according to the phylogenetic tree in *SI Appendix*, Fig. S7). Moreover, two paralogs of *GA 20-oxidase2*, the key enzymes in gibberellin biosynthesis *were up-regulated in* miR156eOE shoot apices in concordance with Gas' effect as a growth-promoting hormone involved in *FT2* regulation (48, 49). Consistently, *GA2-oxidase1*, which encodes an enzyme that inactivates GA, was down-regulated in miR156eOE shoot apices (*SI Appendix*, Fig. S6*C* and Dataset S1*G*). The extensive changes in the expression of genes involved in meristem activity, dormancy regulation, and GA biosynthesis/catabolism pathways in miR156eOE plants suggest that *miR156* may act as a master regulator to integrate various pathways to control growth cessation.

***SPL3/5* Clade Genes Affect Growth Cessation in Hybrid Aspen.** *miR156* functions diversely through regulation of a set of SPL transcription factors. In *Populus*, 28 *SPL* genes were found and grouped into eight major clades, five of which were predicted to have *miR156* recognition sites (*SI Appendix*, Fig. S8 and Table S2). As *SPL* genes play diverse roles largely depending on their spatiotemporal expression patterns (35), we analyzed their year-round expression pattern based on the annual transcriptome data of aspen trees (21). The results showed that *SPL3/5* clade genes peaked in expression during summer and early autumn and partially co-expressed with *FT2* (*SI Appendix*, Fig. S9*A*). Meanwhile, all the *SPL3/5* clade genes except for *SPL3b* were significantly up- or down-regulated in miR156eOE or STTM156 plants, suggesting that these *SPL* genes are regulated by *miR156* at the transcriptional level (*SI Appendix*, Figs. S6*C* and S9*B*). Therefore, we propose that the *SPL3/5* clade of genes might act downstream of *miR156* to regulate growth cessation. Accordingly, we selected *SPL5c* as a representative member from the *SPL3/5* clade and overexpressed it in hybrid aspen trees (SPL5cOE, *SI Appendix*, Fig. S10 *A*–*C*). We compared the growth cessation response in SPL5cOE and WT plants after SD^{14h} treatment. Interestingly, we found that the SPL5cOE transgenic plants ceased growth immediately after transfer to SDs (Fig. 3*A*), with on average only three new leaves formed after the shift, whereas on average, 10 new leaves formed in WT giving a relative leaf formation ratio of 0.3 (Fig. 3*B*). The SPL5cOE transgenic plants had formed buds after 3 wk of SD^{14h} treatment, when the WT had just ceased growth (Fig. 3*C*). To further confirm the function of *SPL5s*, we generated *spl5abc* triple mutant trees, in which expression of all three *SPL5* paralog genes were knocked out using CRISPR-Cas9 gene editing (*SI Appendix*, Fig. S10*D*). Contrary to *SPL5c* overexpressors, all three *spl5abc* lines displayed a significantly delayed growth cessation (Fig. 3*A*), with on average six more leaves formed compared to WT plants giving a relative leaf formation ratio of 1.5 after SD treatment (Fig. 3*B*). After 3 wk of SD^{14h} treatment, *spl5abc* mutants were still in a state of active growth (Fig. 3*C*). These results suggest that *SPL5s* act as positive regulators of growth cessation in hybrid aspen. As *SPL3a* and *SPL3b* genes group in the same clade as *SPL5* and displayed similar expression patterns to *SPL5s*, we also generated *SPL3a* overexpression lines (SPL3aOE) and

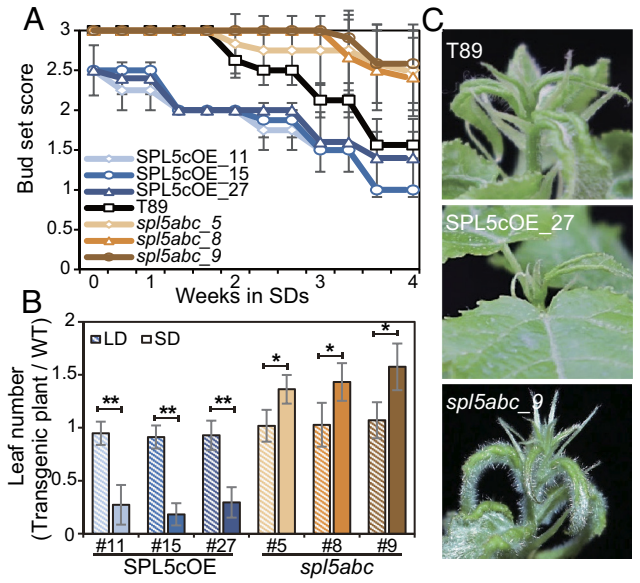

Fig. 3. *SPL3/5* clade genes induce an earlier growth cessation in hybrid aspen. (*A*) Bud set score of SPL5cOE and *spl5abc* lines. (*B*) Leaf initiation ratio of transgenic plants/WT under LD^{18h} and SD^{14h} conditions. Data in (*A*) and (*B*) are mean ± SD (n = 6 to 8). Asterisks denote significant differences of the leaf initiation ratio (transgenic plants/WT) between LD and SD conditions (*$P < 0.05$, **$P < 0.01$; Student's *t* test). (*C*) Representative shoot apex morphologies of T89, SPL5cOE, and *spl5abc* trees 3 wk after SD^{14h} treatment.

checked their growth cessation responses (*SI Appendix*, Fig. S11 *A* and *B*). Like SPL5cOE plants, overexpression of *SPL3a* also induced earlier growth cessation (*SI Appendix*, Fig. S11 *C* and *D*), suggesting that *SPL3/5* clade genes may function cooperatively in controlling growth cessation in *Populus*. Furthermore, plants which overexpressed mir156-resistant versions of *SPL9a* (rSPL9aOE) displayed only minor effects on growth cessation (*SI Appendix*, Fig. S12), suggesting that growth cessation is mainly controlled by *SPL3/5* clade genes.

Genome-Wide Identification of Direct Target Genes of SPL5c. Contrary to the expression pattern of *miR156*, most *SPL3/5* clade genes displayed higher expression levels in the shoot apex compared to their expression levels in the leaf (Fig. 4*A*). To uncover the molecular mechanism of SPL3/5s in growth cessation, we performed Chromatin immunoprecipitation-sequencing (ChIP-seq) analysis to identify genome-wide binding sites of SPL5c using the SPL5cOE line expressing *SPL5c* fused to a 3x Myc epitope tag under the control of the *35S* promoter (35S:SPL5c-MYC). Four independent trials were implemented, and finally, 2,784 putative SPL5c target genes were found to be statistically enriched in at least three trials ($P < 1 \times 10^{-3}$; Dataset S2 *A* and *B*). The binding motifs within the promoters of identified SPL5c potential target genes were analyzed, and the results revealed that the "GTAC" core sequence was enriched in SPL5c binding sites (Fig. 4*B* and *SI Appendix*, Fig. S13), consistent with previous findings that SPL proteins preferentially bind to this core sequence motif (50). Of 2,784 potential targets, 107 and 207 genes were found in miR156eOE RNA-seq DEGs in leaves and shoot apices, respectively, suggesting that these genes are likely to be directly regulated by the miR156-SPL5c module, with 28 genes shared in these two tissues (Fig. 4*C* and Dataset S2*C*). Homologs of many transcription factors that are involved in the regulation of flowering time (*AGAMOUS-LIKE 8*, *SUPPRESSOR OF OVEREXPRESSION OF CONSTANS1LIKE1*, *SVL2*, *SHORT LIFE*), biotic and abiotic responses (*MYB14, MYB55, MYB106, WRKY11, WRKY18, ETHYLENE RESPONSE FACTOR1, SHINE3* etc.), phytohormone signals (*ETHYLENE RESPONSE FACTOR1, CYTOKININ RESPONSE FACTOR2*), and shoot apical meristem maintenance and activity (*BREVIPEDICELLUS1*, *TCP20*) were found to be putative direct targets of SPL5c (*SI Appendix*, Fig. S14). Moreover, one of the *GA 20-oxidase2* (*GA20ox2_1*) genes which was significantly up-regulated in miR156eOE was also found to be a putative direct target of SPL5c (Fig. 4*C* and Dataset S2*C*). We then selected three representative genes (*GA20ox2_1, SVL2*, and *SOC1like1*) that have been reported to be associated with seasonal growth (20, 21, 49) and carried out ChIP with quantitative PCR (ChIP-qPCR) assays (Fig. 4*D*). SPL5c was confirmed to interact with all three loci (Fig. 4*E*). Accordingly, the expression levels of these three genes were up- or down-regulated in miR156eOE, STTM156, and *spl5abc* transgenic plants (Fig. 4*F*). Together, these results suggest that miR156 regulates growth cessation via targeting of SPL3/5 clade genes which integrate multiple pathways.

Age-Dependent Growth Cessation Is Correlated with the Expression of *FT2*. *FT2* is known as the key factor regulating the timing of growth cessation and bud set (1, 24). To investigate whether age-dependent growth cessation is mediated by *FT2*, we compared the expression levels of *FT2* in different ages of trees. Since in *P. tremula FT2* has two duplicated genes (*FT2a* and *FT2b*) with redundant functions in growth cessation and bud set (24), we checked the expression of both *FT2a* and *FT2b*. We first compared the expression level of *FT2a* and *FT2b* between 2-y-old and 4-y-old hybrid poplar leaf samples collected in the field. *Both FT2a* and *FT2b expression* increased with development of the newly produced leaves until they were fully expanded and then declined (Fig. 5 *A* and *B*). Similar expression patterns of *FT2a* and *FT2b* were also found in hybrid aspen grown under controlled conditions (Fig. 5 *C* and *D*). Interestingly, under field conditions, the expression of both *FT2a* and *FT2b* increased earlier in leaves from 2-y-old branches compared to the same position of leaves from 4-y-old branches (Fig. 5 *A* and *B*). This difference was even more obvious between 1st- and 2nd-year-old branches of hybrid aspen trees in controlled conditions (Fig. 5 *C* and *D*). Higher expression levels of *FT2a* and *FT2b* were observed in leaves of 1st branches compared to that in leaves of 2nd-year-old branches (Fig. 5 *C* and *D*). These results suggest that the expression levels of *FT2a* and *FT2b* in developing leaves are regulated by age and that the later growth cessation of juvenile trees may be partially explained by higher expression levels of *FT2a* and *FT2b*.

***miR156* Regulates *FT2* Expression through the Age-Dependent Pathway in Leaves.** To test whether miR156 affects growth cessation and bud set via *FT2*, we first analyzed the expression of *FT2* in different positioned leaves of the first year of miR156eOE or STTM156 plants grown under LD^{18h} conditions. In WT plants, the expression level of both *FT2a* and *FT2b* started to increase in the 6 to 7th leaf, with a peak around the 9 to 11th leaf counted from the newly formed leaves (topmost leaf, "1" in Fig. 5 *E* and *F*). However, the expression levels of *FT2a* and *FT2b* started to increase already from the 4 to 5th leaf in miR156eOE plants (Fig. 5 *E* and *F*). In contrast, the expression of *FT2a* and *FT2b* in STTM156 plants was reduced compared to the WT, with a delayed elevated expression of *FT2a* and *FT2b* until the 11 to 12th leaf (Fig. 5 *E* and *F*). We also analyzed the diurnal expression of *FT2a* and *FT2b* in mature leaves of miR156eOE and STTM156 plants under LD^{18h} conditions. Both *FT2a* and *FT2b* displayed diurnal variations in their expression patterns and were overall upregulated in miR156eOE plants compared to WT plants, whereas in STTM156 plants, the expression of *FT2a* and

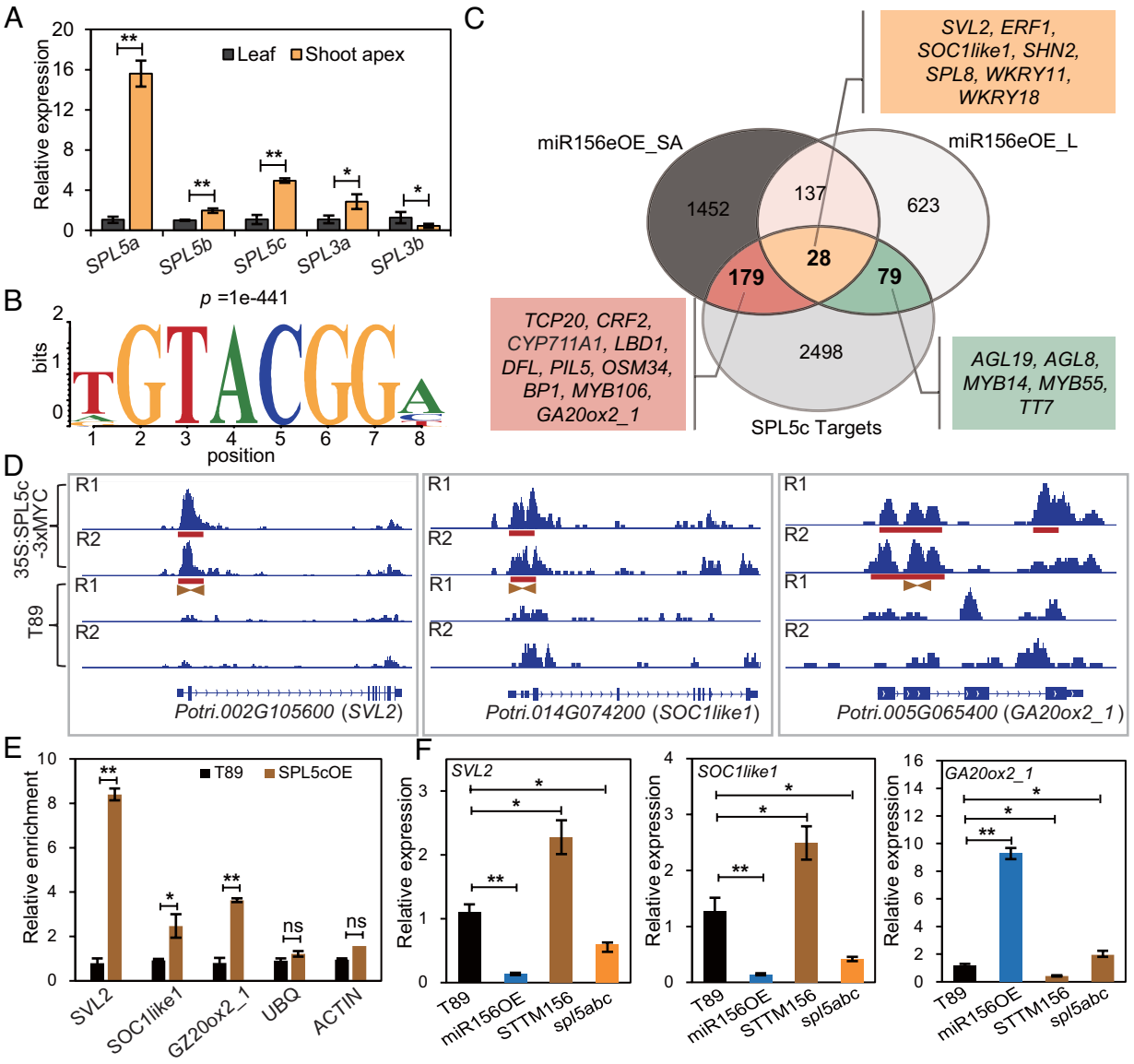

Fig. 4. Identification of direct targets of SPL5c. (*A*) Expression levels and patterns of *SPL3/5* clade genes in leaves and shoot apices of plants growing in LD^{18h} conditions. (*B*) Preferentially bound core sequence from motif analysis of SPL5c-binding peaks. (*C*) Venn diagram showing the common genes among SPL5c direct targets ($P < 1 \times 10^{-3}$) and DEGs in leaves (miR156eOE_L) and shoot apices (miR156eOE_SA) of miR156eOE trees compared to the WT. The representative genes are shown in the colored boxes. (The corresponding *Populus* loc numbers are listed in Dataset S2*C*). (*D*) Binding profiles for selected target genes. The gene structure, name, and locus number are shown at the *Bottom* of each box. The profiles for two experiments (R1 and R2) with the 35S:SPL5c-MYC line are shown in the *Upper* panel, while the two experiments with profiles for T89 are shown in the *Middle* panel. The enriched sites of SPL5c binding are marked with red lines. Primer pairs for ChIP-qPCR are labeled with brown arrows. (*E*) ChIP–qPCR assays validation of SPL5c binding to all three genes shown in Fig. 4*D*. WT plants were used for the ChIP analysis with anti-myc as a control. Enrichment of DNA was calculated as the ratio between 35S:SPL5c-MYC and T89. The DNA fragments of *ACTIN* and *UBIQUITIN* (*UBQ*) genes were used as controls. (*F*) Comparative expression analysis of *SVL2, SOC1like1*, and *GA20ox2_1* in shoot apices of WT, miR156eOE, STTM156 and *spl5abc* lines grown under LD^{18h} conditions. Data shown in (*A*), (*E*) and (*F*) are mean ± SD (n = 3; *$P < 0.05$; **$P < 0.01$; Student's *t* test).

FT2b was reduced to very low levels (Fig. 5 *G* and *H*). Since we found no significant photoperiod responses in the expression of *miR156* either in leaves or shoots (*SI Appendix*, Fig. S5*A*), our results suggest that the *miR156* effects on *FT2* expression might be photoperiod independent. Thus, the combined results of *FT2* expression patterns in different ages of WT trees (Fig. 5 *A*–*D*), and the shifted expression patterns of *FT2* in different ages of leaves in miR156eOE and STTM156 transgenic plants (Fig. 5 *E* and *F*), suggest that *miR156* regulates *FT2* expression through the age-dependent pathway in leaves.

***SPL5c* Directly Suppresses *FT2* Expression.** To explore whether *miR156* regulates *FT2* through its target *SPL3/5s*, we checked the expression level of *FT2a and FT2b* in SPL5cOE and *spl5abc* plants. Expression of both *FT2a* and *FT2b* was significantly repressed in SPL5cOE plants and induced in *spl5abc* plants (Fig. 6 *A* and *B*). We also compared the expression patterns of *FT2a* and *FT2b* in WT plants and *spl5abc* plants in different developing leaves. Consistent with their expression in miR156eOE plants, in *spl5abc* plants, both *FT2a* and *FT2b* displayed an earlier increase in expression with leaf aging (Fig. 6 *A* and *B*). These results indicate that SPL5c might act upstream of *FT2a/b* to repress their expression. Interestingly, we did obtain a significant enrichment of SPL5c binding sites in the *FT2* region in two out of four independent ChIP-seq trials (Dataset S2*A*). We then analyzed the hybrid aspen genomic sequences of *FT2a* and *FT2b* and found multiple putative *SPL5c* binding motifs containing the "GTAC" core sequences. They distributed on promoter and intron regions of both the *FT2a* and *FT2b* loci (Fig. 6*E*). We then performed ChIP-qPCR assays with *FT2a/b* gene-specific and common

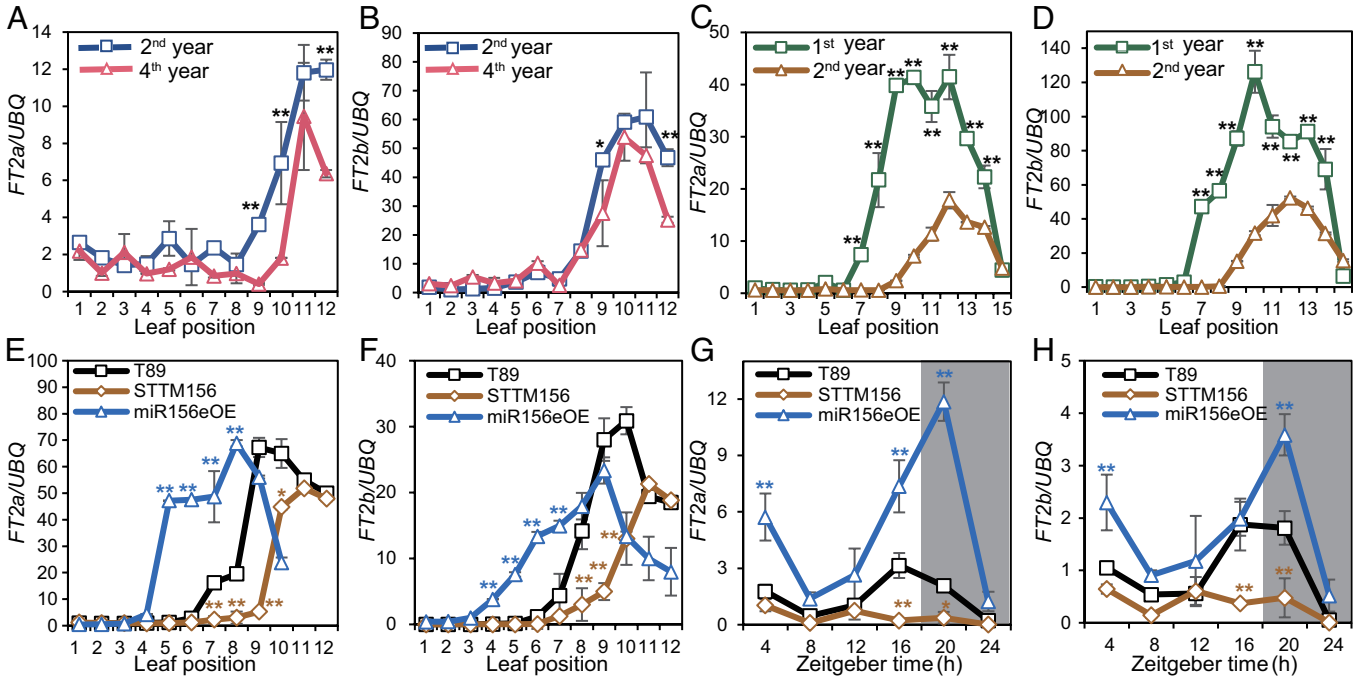

Fig. 5. *miR156* regulates growth cessation by activating *FT2* in leaves through the age-dependent pathway. (*A* and *B*) Expression levels and patterns of *FT2a* and *FT2b* in 2-and 4-y-old hybrid poplar leaves. Samples are the same as in Fig. 1*C*. (*C* and *D*) Expression levels and patterns of *FT2a* and *FT2b* in 1st- and 2nd-year hybrid aspen leaves. Samples are the same as in Fig. 1*F*. (*E* and *F*) Expression levels and patterns of *FT2a* and *FT2b* in T89, miR156eOE, and STTM156 plants. Leaves are counted from the top to the bottom (leaf position, 1 to 12) under LD^{18h} conditions. (*G* and *H*) Diurnal expression analysis of *FT2a* and *FT2b* in mature leaves (leaf 9) of WT, miR156eOE, and STTM156 plants grown under LD^{18h} conditions. Gray boxes indicate night; white boxes indicate day. All data shown in Fig. 5 are mean ± SD (n = 3). ZT, zeitgeber time. Asterisks denote significant differences at a leaf position or a time point between transgenic and WT plants, or comparisons between two different ages of trees (*$P < 0.05$, **$P < 0.01$; Student's *t* test).

primers and detected ~threefold-to-eightfold enrichment in four regions of both the *FT2a* and *FT2b* loci, with the most significant region located 600 bp upstream of the ATG (Fig. 6*F*). Since the putative SPL5c target sites of *FT2a* and *FT2b* were conserved, we then focused on this location in *FT2a* (P1) and performed in vitro yeast one-hybrid (Y1H) assays. The result clearly showed that SPL5c can bind to this promoter region of *FT2a* (Fig. 6*G*). Electrophoretic mobility shift assays (EMSAs) were performed to further confirm its binding. We designed a probe in the P1 region predicted to have a putative SPL5c binding sites (GTAC motif, corresponding to amplicon aT5 in Fig. 6*E*). GST-SPL5c displayed a gel shift with this probe, while no shift was observed for GST-SPL5c when the predicted SPL5c-binding sites were mutated or after addition of unlabeled probe competitors (Fig. 6*H*). Therefore, in vitro and in vivo evidence together supported that SPL5c can bind directly to the promoter of *FT2*. The influence of SPL5c on the *FT2a* promoter activity was tested with a dual-luciferase reporter assay (Fig. 6*I*). The results indicated that SPL5c could significantly repress the *FT2a* promoter activity (Fig. 6 *J* and *K*). Taken together, these results show that SPL5c can bind directly to the *FT2* promoter to repress its expression.

Discussion

In forests, juvenile tree seedlings often display longer growth seasons compared to adult trees, an adaptive strategy to ensure juvenile seedling establishment and survival under canopy shade (28–30, 51). This phenomenon is genetically regulated as differences in growth cessation among different ages of trees can be observed under both natural field and artificial controlled growth conditions (Fig. 1). In this study, we report the identification of putative regulators and the molecular framework that mediate age-dependent growth cessation in hybrid aspen. We find that the *miR156-SPL* module, a key regulon of VPC in poplar, also triggers age-dependent growth cessation in hybrid aspen. We propose a model for how the *miR156-SPL* module integrates multiple pathways to regulate seasonal growth cessation in hybrid aspen (Fig. 7). According to this model, the *miR156-SPL* module regulates growth cessation through various pathways in leaves, and/or in shoot apices, with at least three pathways meriting discussion and further investigation. First, *SPL3/5s* inhibits growth by directly repressing the expression of *FT2*, which is the key gene responsive to daylength in leaves and is necessary to keep the shoot apex in active growth. Second, *SPL3/5s* might inhibit meristem activity locally in shoot apices by modifying meristem maintenance genes, such as *STM* and *CLEs*. And third, *SPL3/5s* may suppress growth by repressing *GA 20-oxidase2 expression to inhibit* the GA synthetic pathway directly or indirectly through *SVP/AGL24-like* genes. Besides *SVL*, other *SVP/AGL24-like* genes have also been supposed to play roles in tree vegetative growth phenology (21), although the genetic evidence is still lacking (*SI Appendix*, Fig. S7). Moreover, we also propose a possible flowering onset role of the *miR156-SPL* module, as many *Populus* orthologs of flowering genes were found to be putative direct targets of SPL5c (Fig. 7). The *miR156-SPL* module has been implicated in the regulation of flowering in both the perennial herb *Arabis alpina* (52) and the conifer tree *Picea abies* (53). To what extent the *miR156-SPL* module regulates flowering onset in *Populus* merits further investigation. In addition, earlier spring bud breaks have been reported in juvenile stages of many tree species, which is another factor which is important to extend the growing season to ensure seedling establishment and long-term survival (51). Interestingly, we found that altered expression of miR156 also affects bud break (*SI Appendix*, Fig. S4), suggesting that it can act to regulate both the start and the end of the growing season during the seasonal growth cycle. How *miR156* and its

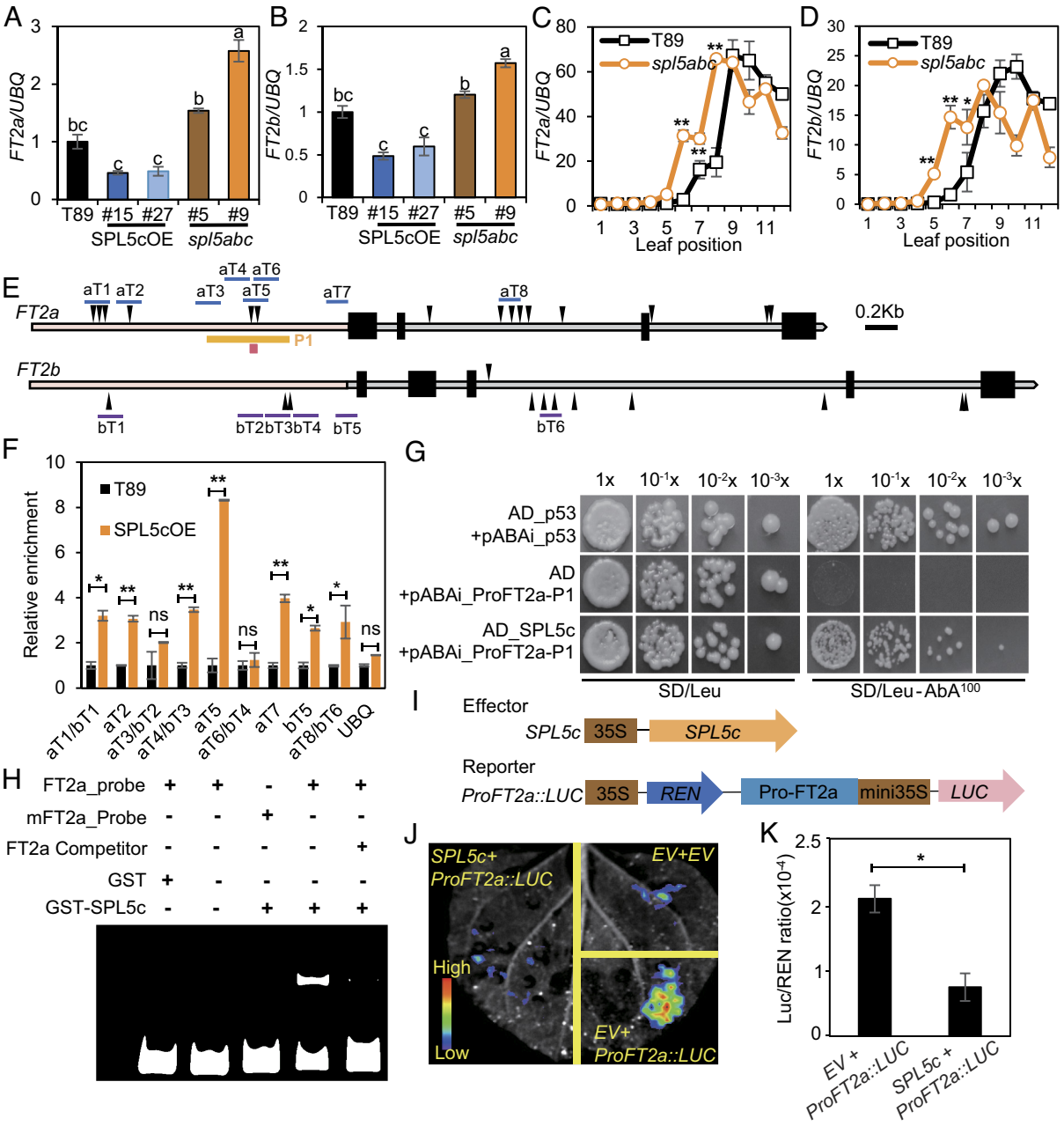

Fig. 6. SPL5c directly represses *FT2a* and *FT2b* expression in the leaf. (*A* and *B*) Quantitative levels of *FT2a* and *FT2b* transcripts in T89, SPL5cOE, and *spl5abc* trees. The 8th to 10th mature leaves from the top were collected. Data are mean ± SD (n = 3). Different letters represent significant differences from each other as determined by one-way ANOVA with Tukey's multiple comparisons test, $P < 0.05$. (*C* and *D*) Expression levels and patterns of *FT2a* and *FT2b* in T89 and *spl5abc* trees. Leaves from the top to the bottom (leaf order, 1 to 12) were collected under LD^{18h} conditions. Data are mean ± SD (n = 3; $^*P < 0.05$, $^{**}P < 0.01$; Student's *t* test). (*E*) Schematic diagram of the SPL5c binding motifs (black triangles) in the *FT2a* and *FT2b* loci, the amplicon locations for the ChIP-qPCR analysis, the fragment for yeast one hybrid (yellow box) and probes for EMSA (red box). Black boxes represent exons. (*F*) ChIP-qPCR assay showing *FT2a* and *FT2b* chromatin regions associate with SPL5c. Due to the high sequence homology of *FT2a* and *FT2b*, many amplicons can match both genes. Plants were harvested under LD^{18h} conditions. The *UBQ* gene amplicon was used as control ($^*P < 0.05$; $^{**}P < 0.01$; Student's *t* test). Error bars ± SD (n = 3). ns, no significant difference. (*G*) Yeast one-hybrid assay showing that SPL5c directly binds to the *FT2a* promoter. AD-p53/pABAi-p53 was used as a positive control. (*H*) EMSA showing that GST-SPL5c binds to the DY680-labeled *FT2a* probe containing the GTAC motif. The DNA-binding capacity of the protein disappeared when a mutated DNA probe missing the SPL-binding sites was used. Unlabeled *FT2a* probes were used as competitors. (*I*) Schematic representation of the effector and reporter constructs used for transient expression assay in (*J*) and (*K*). *SPL5c* under the control of the *35S* promoter was used as the effector. The firefly luciferase gene *LUC* driven by the *FT2a* promoter and the Renilla luciferase gene *REN* under the control of the *35S* promoter were used as the reporter and internal control respectively. (*J*) and (*K*) Transient expression assay showing that *SPL5c* trans-repressed *FT2a* expression in *Nicotiana benthamiana* leaves. Data are normalized to the internal control *35S::REN*. All data are means ± SD (n = 3). Asterisks denote significant differences between combinations ($^*P < 0.05$; Student's *t* test). EV, empty vector.

targets *SPLs* spatiotemporally regulate the seasonal growth events is also worthy of further investigation. To our surprise, *miR156* regulates growth cessation by increasing the expression of *FT2*, which is known to play dual roles in both growth cessation inhibition and flowering promotion in *Populus* (1, 2). That is contradictory to the notion from the *Arabidopsis* model where *miR156* is a repressor of *FT* expression (54, 55). In *Arabidopsis*, *SPL* genes are activators of flowering through an indirect activation of *FT* expression in leaves (54, 55) or by directly activating flower meristem identity genes downstream of *FT* in the shoot apex (45). In our study, we show that *SPL3/5s* repress the expression of *FT2* by directly binding to its promoter in leaves. The opposite effect

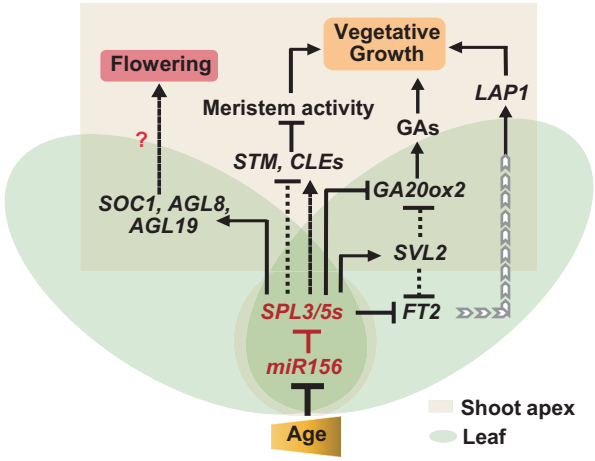

Fig. 7. Working model of the *miR156-SPL3/5s* module in the control of age-dependent growth cessation in hybrid aspen. The *miR156-SPL* module acts as a regulatory hub that connects the internal age signal to the tree's seasonal growth activity. *miR156* promotes active vegetative growth, while *SPL3/5s* repress it. The *miR156-SPL* module regulates seasonal growth through various pathways. *SPL3/5s* inhibit growth by directly repressing the expression of *FT2* in the leaf as well as by repressing *GA 20-oxidase2* directly, or indirectly through *SVL2* both in the leaf and shoot apex. *SPL3/5s* may also inhibit meristem activity locally in the shoot apex by modifying the expression of meristem maintenance genes, such as *STM* and *CLEs*. Moreover, the *miR156-SPL* module may control flowering onset through a couple of *MADS-box* flowering genes. Solid lines represent direct genetic interactions or verified effects on growth processes. Dotted lines and question marks represent connections that need to be characterized further.

of the miR156/*SPL/FT* regulon in *Populus* suggests that perennial trees might have evolved different mechanisms to coordinate the miR156-*SPL* module into different development processes that are quite different from annual plants. Second, the age-dependent growth cessation phenomenon seems to occur only in very early juvenile development as no growth cessation difference was observed among 4-, 6-, and 10-y-old-field planted hybrid poplar (Fig. 1 *A* and *B*). Interestingly, a recent study of VPC in hybrid poplar suggests that the poplar VPC completes at an early stage of development as the onset of adult traits already begins within 3 mo of seedling growth (34), yet the first floral induction in many *Populus* species does not occur until after at least 4 to 5 y of vegetative growth. Thus, we speculate that the age-dependent growth cessation is accompanied by VPC in *Populus* at an early tree age when the flowering induction has yet not been initiated. *Populus FT* and *TFL1* family genes have evolved to coordinate the flowering regulation and the seasonal vegetative growth processes (25). This strategy largely depends on the spatiotemporal expressions of these genes (25). In our study, the declined expression of *FT2* is tightly related to VPC, while its expression is relatively stable in different ages of adult trees. Thus, the seemingly contradictory effects of the *miR156-SPL3/5s* module on *FT2* expression in growth cessation and flowering in hybrid aspen may be due to differences in its spatiotemporal expression.

In annual plants, the *miR156-SPL* module has been widely studied and functions in multiple pathways during different ages and stages of plant development (47). In our study, besides its roles in tree phenology, the global gene changes in miR156eOE plants and the wide targets of SPL5c obtained from ChIP-seq data suggest that the *miR156-SPL3/5s* module in *Populus* might have multiple other roles (*SI Appendix*, Fig. S6*C* and Fig. 4*C*), such as trichome development, anthocyanin biosynthesis, wax biosynthesis, biotic and abiotic responses, etc. However, one must bear in mind that these functions might be overestimated since they are based on experiments in overexpression plants. Particularly, the *miR156-SPL* module might play important roles in biotic and abiotic stress response in trees as a huge number of stress-related genes were changed in response to the expression level of *miR156* (*SI Appendix*, Fig. S6 *A* and *C*). This is reasonable as seedling establishment and juvenile growth are critical stages for tree survival in natural forests. Multiple strategies including seasonal phenology patterns and bio- and abiotic responses have co-evolved to make sure seedlings survive and establish their growth in a highly competitive and harsh forest environment. Further investigation of the *miR156-SPL* module in trees will help us to better understand the survival strategy of perennial trees and how they adapt to changes in their environment, including climate change.

Materials and Methods

Plant materials, plant phenotyping, grafting assay, vector construction, genetic transformation, transgene phenotyping, ChIP assay, RNA-sequencing, bioinformatic analysis, RNA quantification, yeast one-hybrid assay, EMSA, and dual-luciferase transcriptional activity assay are described in detail in *SI Appendix*, Materials and Methods. Primer sequences are listed in *SI Appendix*, Table S3.

Data, Materials, and Software Availability. The data that support the findings of this study are available within the paper and its supporting information. Raw sequencing data are available in the Sequence Read Archive at the National Center for Biotechnology Information (NCBI) Center with the accession number PRJNA973968 and PRJNA974156. The aspen year-round RNA-seq data were obtained from the European Nucleotide Archive under the accession number PRJEB46749 (21).

ACKNOWLEDGMENTS. This work was supported by the National Natural Science Foundation of China (32271824 and 31971676) and the Fundamental Research Funds for the Central Universities (2662019PY007) to J.D. and by the Swedish Research Council, the Knut and Alice Wallenberg Foundation and the Swedish Governmental Agency for Innovation Systems (VINNOVA) to O.N. The computations in this paper were run on the bioinformatics computing platform of the National Key Laboratory of Crop Genetic Improvement, Huazhong Agricultural University.

1. H. Bohlenius *et al.*, CO/FT regulatory module controls timing of flowering and seasonal growth cessation in trees. *Science* **312**, 1040–1043 (2006).
2. C. Y. Hsu *et al.*, FLOWERING LOCUS T duplication coordinates reproductive and vegetative growth in perennial poplar. *Proc. Natl. Acad. Sci. U.S.A.* **108**, 10756–10761 (2011).
3. J. H. Ding, O. Nilsson, Molecular regulation of phenology in trees–because the seasons they are a-changin'. *Curr. Opin. Plant Biol.* **29**, 73–79 (2016).
4. J. Wang, J. Ding, Molecular mechanisms of flowering phenology in trees. *Forestry Res.* **3**, 2 (2023), 10.48130/FR-2023-0002.
5. J. Ding, B. Zhang, Y. Li, D. Andre, O. Nilsson, Phytochrome B and PHYTOCHROME INTERACTING FACTOR8 modulate seasonal growth in trees. *New Phytol.* **232**, 2339–2352 (2021).
6. I. Kozarewa *et al.*, Alteration of PHYA expression change circadian rhythms and timing of bud set in Populus. *Plant Mol. Biol.* **73**, 143–156 (2010).
7. J. Ding *et al.*, GIGANTEA-like genes control seasonal growth cessation in Populus. *New Phytol.* **218**, 1491–1503 (2018).
8. J. M. Ramos-Sanchez *et al.*, LHY2 integrates night-length information to determine timing of poplar photoperiodic growth. *Curr. Biol.* **29**, 2402–2406.e4 (2019).
9. S. Tylewicz *et al.*, Dual role of tree florigen activation complex component FD in photoperiodic growth control and adaptive response pathways. *Proc. Natl. Acad. Sci. U.S.A.* **112**, 3140–3145 (2015).
10. X. Sheng, C. Y. Hsu, C. Ma, A. M. Brunner, Functional diversification of Populus FLOWERING LOCUS D-LIKE3 transcription factor and two paralogs in shoot ontogeny, flowering, and vegetative phenology. *Front Plant Sci.* **13**, 805101 (2022).
11. A. Azeez, P. Miskolczi, S. Tylewicz, R. P. Bhalerao, A tree ortholog of APETALA1 mediates photoperiodic control of seasonal growth. *Curr. Biol.* **24**, 717–724 (2014).
12. A. Karlberg, L. Bako, R. P. Bhalerao, Short day-mediated cessation of growth requires the downregulation of AINTEGUMENTALIKE1 transcription factor in hybrid aspen. *PLoS Genet.* **7**, e1002361 (2011).
13. S. Tylewicz *et al.*, Photoperiodic control of seasonal growth is mediated by ABA acting on cell-cell communication. *Science* **360**, 212–214 (2018).
14. S. Jimenez, A. L. Lawton-Rauh, G. L. Reighard, A. G. Abbott, D. G. Bielenberg, Phylogenetic analysis and molecular evolution of the dormancy associated MADS-box genes from peach. *BMC Plant Biol.* **9**, 81 (2009).

15. H. Yu, Y. Xu, E. L. Tan, P. P. Kumar, AGAMOUS-LIKE 24, a dosage-dependent mediator of the flowering signals. *Proc. Natl. Acad. Sci. U.S.A.* **99**, 16336–16341 (2002).
16. J. H. Lee *et al.*, Role of SVP in the control of flowering time by ambient temperature in Arabidopsis. *Genes Dev.* **21**, 397–402 (2007).
17. R. M. Wu *et al.*, Conservation and divergence of four kiwifruit SVP-like MADS-box genes suggest distinct roles in kiwifruit bud dormancy and flowering. *J. Exp. Bot.* **63**, 797–807 (2012).
18. V. da Silveira Falavigna *et al.*, Unraveling the role of MADS transcription factor complexes in apple tree dormancy. *New Phytol.* **232**, 2071–2088 (2021).
19. R. Sasaki *et al.*, Functional and expressional analyses of PmDAM genes associated with endodormancy in Japanese apricot. *Plant Physiol.* **157**, 485–497 (2011).
20. V. D. S. Falavigna, B. Guitton, E. Costes, F. Andres, I want to (Bud) break free: The potential role of DAM and SVP-Like genes in regulating dormancy cycle in temperate fruit trees. *Front. Plant Sci.* **9**, 1990 (2018).
21. D. Andre *et al.*, Populus SVL acts in leaves to modulate the timing of growth cessation and bud set. *Front. Plant Sci.* **13**, 823019 (2022).
22. R. K. Singh *et al.*, A genetic network mediating the control of bud break in hybrid aspen. *Nat. Commun.* **9**, 4173 (2018).
23. R. K. Singh, P. Miskolczi, J. P. Maurya, R. P. Bhalerao, A tree ortholog of SHORT VEGETATIVE PHASE floral repressor mediates photoperiodic control of bud dormancy. *Curr. Biol.* **29**, 128–133.e2 (2019).
24. D. Andre *et al.*, FLOWERING LOCUS T paralogs control the annual growth cycle in Populus trees. *Curr. Biol.* **32**, 2988–2996 (2022).
25. X. Sheng, R. A. Mahendra, C. T. Wang, A. M. Brunner, CRISPR/Cas9 mutants delineate roles of Populus FT and TFL1/CEN/BFT family members in growth, dormancy release and flowering. *Tree Physiol.* **43**, 1042–1054 (2023).
26. D. Weigel, O. Nilsson, A developmental switch sufficient for flower initiation in diverse plants. *Nature* **377**, 495–500 (1995).
27. H. Thomas, Ageing in plants. *Mech. Ageing Dev.* **123**, 747–753 (2002).
28. K. Seiwa, Ontogenetic changes in leaf phenology of Ulmus davidiana var. japonica, a deciduous broad-leaved tree. *Tree Physiol.* **19**, 793–797 (1999).
29. D. S. Gill, J. S. Amthor, F. H. Bormann, Leaf phenology, photosynthesis, and the persistence of saplings and shrubs in a mature northern hardwood forest. *Tree Physiol.* **18**, 281–289 (1998).
30. J. E. Cooke, M. E. Eriksson, O. Junttila, The dynamic nature of bud dormancy in trees: Environmental control and molecular mechanisms. *Plant Cell Environ.* **35**, 1707–1728 (2012).
31. S. Yu, H. Lian, J. W. Wang, Plant developmental transitions: The role of microRNAs and sugars. *Curr. Opin. Plant Biol.* **27**, 1–7 (2015).
32. J. W. Wang *et al.*, MiRNA control of vegetative phase change in trees. *PLoS Genet.* **7**, e1002012 (2011).
33. L. Yang, S. R. Conway, R. S. Poethig, Vegetative phase change is mediated by a leaf-derived signal that represses the transcription of miR156. *Development* **138**, 245–249 (2011).
34. E. H. Lawrence *et al.*, Vegetative phase change in Populus tremula x alba. *New Phytol.* **231**, 351–364 (2021).
35. M. Xu *et al.*, Developmental functions of miR156-regulated SQUAMOSA PROMOTER BINDING PROTEIN-LIKE (SPL) genes in Arabidopsis thaliana. *PLoS Genet.* **12**, e1006263 (2016).
36. X. Chen *et al.*, SQUAMOSA promoter-binding protein-like transcription factors: Star players for plant growth and development. *J. Integr. Plant Biol.* **52**, 946–951 (2010).
37. M. J. Aukerman, H. Sakai, Regulation of flowering time and floral organ identity by a MicroRNA and its APETALA2-like target genes. *Plant Cell* **15**, 2730–2741 (2003).
38. G. Wu *et al.*, The sequential action of miR156 and miR172 regulates developmental timing in Arabidopsis. *Cell* **138**, 750–759 (2009).
39. L. Yang, M. Xu, Y. Koo, J. He, R. S. Poethig, Sugar promotes vegetative phase change in Arabidopsis thaliana by repressing the expression of MIR156A and MIR156C. *Elife* **2**, e00260 (2013).
40. J. Gao *et al.*, A robust mechanism for resetting juvenility during each generation in Arabidopsis. *Nat. Plants* **8**, 257–268 (2022).
41. S. Yu *et al.*, Sugar is an endogenous cue for juvenile-to-adult phase transition in plants. *Elife* **2**, e00269 (2013).
42. J. W. Wang, R. Schwab, B. Czech, E. Mica, D. Weigel, Dual effects of miR156-targeted SPL genes and CYP78A5/KLUH on plastochron length and organ size in Arabidopsis thaliana. *Plant Cell* **20**, 1231–1243 (2008).
43. G. T. Howe, W. P. Hackett, G. R. Furnier, R. E. Klevorn, Photoperiodic responses of a northern and southern ecotype of black cottonwood. *Physiol. Plant.* **93**, 695–708 (1995).
44. P. Miskolczi *et al.*, Long-range mobile signals mediate seasonal control of shoot growth. *Proc. Natl. Acad. Sci. U.S.A.* **116**, 10852–10857 (2019).
45. J. W. Wang, B. Czech, D. Weigel, miR156-regulated SPL transcription factors define an endogenous flowering pathway in Arabidopsis thaliana. *Cell* **138**, 738–749 (2009).
46. G. Wu, R. S. Poethig, Temporal regulation of shoot development in Arabidopsis thaliana by miR156 and its target SPL3. *Development* **133**, 3539–3547 (2006).
47. J. W. Wang, Regulation of flowering time by the miR156-mediated age pathway. *J. Exp. Bot.* **65**, 4723–4730 (2014).
48. M. E. Eriksson, M. Israelsson, O. Olsson, T. Moritz, Increased gibberellin biosynthesis in transgenic trees promotes growth, biomass production and xylem fiber length. *Nat. Biotechnol.* **18**, 784–788 (2000).
49. M. E. Eriksson, D. Hoffman, M. Kaduk, M. Mauriat, T. Moritz, Transgenic hybrid aspen trees with increased gibberellin (GA) concentrations suggest that GA acts in parallel with FLOWERING LOCUS T2 to control shoot elongation. *New Phytol.* **205**, 1288–1295 (2015).
50. H. Pei *et al.*, Low-affinity SPL binding sites contribute to subgenome expression divergence in allohexaploid wheat. *Sci. China Life Sci.* **66**, 819–834 (2022).
51. C. K. Augspurger, E. A. Bartlett, Differences in leaf phenology between juvenile and adult trees in a temperate deciduous forest. *Tree Physiol.* **23**, 517–525 (2003).
52. Y. Hyun *et al.*, A regulatory circuit conferring varied flowering response to cold in annual and perennial plants. *Science* **363**, 409–412 (2019).
53. S. Akhter *et al.*, Cone-setting in spruce is regulated by conserved elements of the age-dependent flowering pathway. *New Phytol.* **236**, 1951–1963 (2022).
54. J. J. Kim *et al.*, The microRNA156-SQUAMOSA PROMOTER BINDING PROTEIN-LIKE3 module regulates ambient temperature-responsive flowering via FLOWERING LOCUS T in Arabidopsis. *Plant Physiol.* **159**, 461–478 (2012).
55. J. Mathieu, L. J. Yant, F. Murdter, F. Kuttner, M. Schmid, Repression of flowering by the miR172 target SMZ. *PLoS Biol.* **7**, e1000148 (2009).